This article has been accepted for publication in a future issue of this journal, but has not been fully edited. Content may change prior to final publication. Citation information: DOI 10.1109/JLT.2016.2636442, Journal of Lightwave Technology

Demonstration of 16QAM-OFDM UDWDM Transmission Using a Tunable Optical Flat Comb Source

Abir Hraghi, *Student Member, IEEE,* Mohamed Essghair Chaibi, *Student Member, IEEE,* Mourad Menif, *Member, IEEE,* and Didier Erasme, *Member, IEEE,*

***Abstract*—A new approach for designing broad and flattened spectrum multicarriers optical sources is presented leading to a 32 spectral lines source using a dual-arm Mach-Zehnder modulator (MZM) and a 41 spectral lines source from two-stage MZM. A modified simulated annealing-based optimization method is applied to derive the necessary settings allowing the optical flat comb source (OFCS) to be ultraflat. The OFCS is mooted as a technology to enhance the overall capacity of an access optical network by increasing the number of WDM channels. Here, we demonstrate an ultra-dense WDM (UDWDM) transmission for application to passive optical networks (PON) with ($11\times12.5Gbps$) Quadrature Amplitude Modulation (QAM) based on a 4b/s/Hz spectral efficiency orthogonal frequency division multiplex (16QAM-OFDM) transmitter and direct detection. We use an OFCS to generate the 11 subcarriers spaced by 6.25GHz, made of a two-stage MZM. We study the performance of 3 filtered channels in terms of error vector magnitude (EVM) in back-to-back (B-to-B) conditions and after propagation through 25km and 100km standard single mode fiber (SSMF).**

***Index Terms*—UDWDM-PON, Optical Flat Comb Source, OFDM, direct detection, Dual arm-MZM.**

I. Introduction

THE optical industry is working actively to derive new techniques to increase the total capacity of the deployed optical networks in order to meet the unprecedented growth of Internet traffic induced by the emerging hungry bandwidth applications [1]. New solutions have to be low-cost, easily implemented, and scalable.

The next generation passive optical network 2 (NG-PON 2), have been designed in order to increase the bit-rate thus making a large stride toward a high-performance, low-overhead optical interconnect infrastructure [2]. In 2015, the NG-PON2 allows 40Gbps downstream and 10Gbps upstream capacity with an extended range (ER) up to 60km. Wavelength division multiplexing (WDM) is the solution adopted to obtain bit rate enhancement. The WDM solution is resilient to channel impairments such as chromatic dispersion. Increasing the overall capacity may go through increasing the number of WDM channels while keeping the same bit-rate per channel. Therefore, the WDM-PON presents an appropriate technology which will be used as the next generation network. In order to achieve a high bit rate, increasing the number of WDM channels has attracted considerable attention. Therefore, research efforts oriented toward the exploration and development of ultra-dense WDM-PON (UDWDM-PON). Today, research on coherent UDWDM-PON seems more important and interesting with the use of advanced modulation formats quadrature phase shift keying (QPSK) and quadrature amplitude modulation based on 16 (16QAM)) and multiplexing techniques (Nyquist pulse shape and orthogonal frequency division multiplexing (OFDM)) [3]–[5]. However, many standards conserve a direct detection-reception scheme due to the simplicity and the low cost of this technique compared to the coherent solution [6]–[8].

A complete infrastucture in the UWDM-PON is adapted by providing a separate wavelength domain in the uplink and the downlink transmissions for each user [9]. It can cope with future bandwidth demand due to the allocation of separate bandwidth. However, high capacity UDWM-PON requires a large number of laser sources at the optical line terminal (OLT) side thus increasing the complexity of the transmitter in terms of size and costs. In addition, an array of single mode lasers is difficult to use because of the need for a line-by-line frequency control. Known for its small size and low cost, an optical flat comb source can be used as a source at the OLT and replace a conventional setup in WDM-PON. Several works investigated the use of an optical comb source [10], [11]. In addition, the comb source can be used both for downstream and upstream transmissions in the case when the optical network units (ONU) use a component reflecting and modulating a wavelength generated at the optical line terminal.

A flat optical comb source allows the same optical budget for all wavelengths. This is an important feature as all ONUs are supposed to operate with all the wavelengths existing in the network. Various techniques in the generation of frequency comb sources have been reported including supercontinuum and mode locked lasers [12], [13]. However those methods either need special manufacturing or are prohibitively expensive. Therefore, electro-optical modulators have received considerable attention.

In this paper, we performed two main contributions. Fist, a new approach for designing broad and flattened spectrum multicarriers optical sources is presented leading to a 32 spectral lines source using a dual-arm Mach-Zehnder modulator (MZM) and a 41 spectral lines source from two-stage

A. Hraghi, and M. Menif, are with GRESCOM Laboratory, Higher School of Communications of Tunis (Sup'Com), University of Carthage, City of Communications Technologies, 2083 Ariana, Tunisia (e-mail: abir.hraghi@supcom.tn; mourad.mnif@supcom.tn).

M. E. Chaibi and D. Erasme are with Télécom ParisTech - CNRS LTCI, 46 rue Barrault, F-75634 Paris Cedex 13, France (e-mail:chaibi@telecom-paristech.fr; didier.erasme@telecom-paristech.fr).

This article has been accepted for publication in a future issue of this journal, but has not been fully edited. Content may change prior to final publication. Citation information: DOI 10.1109/JLT.2016.2636442, Journal of Lightwave Technology

MZM. A modified simulated annealing-based optimization method is applied to derive the necessary settings allowing the optical flat comb source (OFCS) to be ultraflat. Second, We introduce a versatile technique for tightly space OFCS, which is implemented at the side of OLT to achieve high capacity in next generation UDWM-PON systems. we demonstrate a long-reach UDWDM-PON based on 16QAM-OFDM modulation and direct detection. A tunable optical flat comb source (OFCS) consisting of a two-stage Mach-Zehnder modulator (MZM) is used in order to generate eleven 6.25GHz-spaced subcarriers exhibiting a spectral ripple below 1dB. Each subcarrier is modulated by a 12.5Gbps 16QAM-OFDM signal. We evaluated the performance of 3 filtered channels in terms of error vector magnitude (EVM) in back-to-back (B-to-B) and over 25km and 100km standard single mode fibers (SSMF). The remainder of this paper is organized as follows. In section II, the techniques used for generating the optical flat comb source is described. The experimental setup for OFCS generation is presented in section III. 16QAM-OFDM UDWDM PON using a tunable optical flat comb source is proposed in section IV. Finally, the conclusions are given in section V.

II. Optical Flat Comb Source Generation

A. Case of a dual arm Mach-Zehnder modulator

Several techniques have been used in order to generate a frequency comb source based on electro-optical modulator. A cascade mounted MZMs were used by Wu *et al.* to make frequency comb source [14], and dual parallel MZMs were used by Gheorma *et al.* [15]. In the case of Yiran Ma *et al.* [16] an optical I/Q modulator followed by an erbium doped fiber amplifier (EDFA) led to the generation of an ultra-flat comb source. Recently, Wiemann *et al.* [17] demonstrated a silicon organic hybrid (SOH) electro-optic modulator based scheme. As mentioned in the works of Zhou *et al.* [18], Zhang *et al.* [19], and Chen *et al.* [20], the use of more than a single modulator for optical frequency comb generation is a common theme. The use of a single dual arm MZM makes the method of Sakamodo *et al.* much more advantageous in terms of cost than the others techniques [21]. The frequency comb source generated using a single dual arm MZM is characterized by an excellent spectral flatness and a low noise.

Fig.1 illustrates the configuration of OFCS based on a dual arm Mach-Zehnder modulator (DA-MZM). Each arm of the DA is DC biased and driven by an RF sinusodal signal $S_1(t)$ and $S_2(t)$. These two signals are in-phase. The induced phase shift in each arm is respectively:

$$\phi_1(t) = \theta_1 + A_1 sin(\omega t) \tag{1}$$

$$\phi_2(t) = \theta_2 + A_2 sin(\omega t) \tag{2}$$

where θ_1 and θ_2 are the static phase-shifts induced by the DC biases and A_1 and A_2 the amplitude of the phase-shifts induced by RF signals S_1 and S_2.

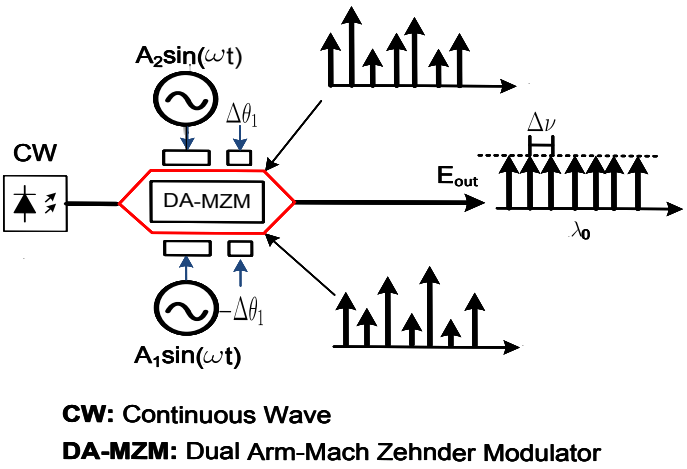

Fig. 1. Optical flat comb source based on DA-MZM

The subcarrier spacing is defined by $\Delta\nu$, where $\Delta\nu = \omega/2\pi$. The optical field at the output of the MZM is given by the following equation [21].

$$E_{out} = \frac{E_{in}}{2} \sum_{k=-\infty}^{+\infty} \left[J_k(A_1) e^{j(k\omega t + \theta_1)} + J_k(A_2) e^{j(k\omega t + \theta_2)} \right] \tag{3}$$

with E_{in} the input power of a continuous wave (CW) laser, J_k the k^{th} order of first kind of Bessel function, A_1 and A_2 the amplitude of the driving sine-waves $S_1(t)$ and $S_2(t)$, respectively. The power conversion from the CW input to each harmonic mode can be asymptotically approximated as [21]:

$$\eta = \frac{P_k}{P_{in}} = \frac{1}{2\pi\bar{A}} \left[1 + cos(\Delta\theta) cos(2\Delta A) + \{cos(2\Delta\theta) + cos(2\Delta A)\} cos\left\{ 2\bar{A} - \frac{2k+1}{2} \right\} \right] \tag{4}$$

where $\Delta A = (A_1 - A_2)/2$, $\Delta\theta = (\theta_1 - \theta_2)/2$ and $\bar{A} = (A_1 + A_2)/2$ are the peak to peak phase difference induced in each arm of the MZM, the DC bias difference between the arms and the average amplitude, respectively. The condition $\Delta A + \Delta\theta = n\pi \pm \pi/2$ must be satisfied, in order to obtain an OFCS leading to $\bar{A} = 4\pi$, $\Delta A = 0.125\pi$ and $\Delta\theta = 0.375\pi$, as mentioned in [21]. The flatness condition proposed by Sakamoto *et al.* is described by the following equation:

$$\Delta A \pm \Delta\theta = \frac{\pi}{2} \tag{5}$$

The bandwidth of the output spectrum is limited to 11 subcarriers with 1.1dB spectral ripple, as depicted in Fig.2. It must be pointed out that the spectrum resulting from the aforementioned condition does not take into account the physical aspect of the output spectrum i.e. the limited bandwidth of the modulator and of its driver. In order to obtain a superflat OFCS, we will introduce two new parameters in the following section, namely the number of the flat harmonic N_{flat} and the spectral ripple ΔP to the flatness condition.

B. Case of two-stage Mach-Zehnder modulator

In this subsection, a scheme based on a cascade of dual arm and push-pull Mach-Zehnder modulators is demonstrated

This article has been accepted for publication in a future issue of this journal, but has not been fully edited. Content may change prior to final publication. Citation information: DOI 10.1109/JLT.2016.2636442, Journal of Lightwave Technology

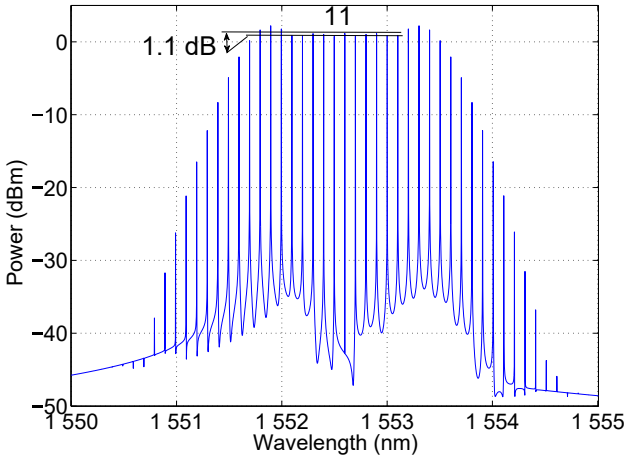

Fig. 2. Symmetrical output spectrum ($A_1 = 23\pi/4$, $A_2 = 25\pi/4$ and $\Delta\theta = \pi/4$)

in order to generate an OFCS characterized by a very high spectral flatness. The output optical spectrum emanating from a dual arm MZM is expressed as follows, in the case of synchronous sine-wave excitation by $S_1(t) = A_1 \sin(\omega_1 t)$ and $S_2(t) = A_2 \sin(\omega_1 t)$ is:

$$\begin{aligned} E_{out} &= \frac{1}{2} E_{in} \sum_{k=-\infty}^{+\infty} \left[J_k(A_1) e^{j(k\omega_1 t + \theta_1)} + J_k(A_2) e^{j(k\omega_1 t - \theta_2)} \right] \\ &= \frac{1}{2} E_{in} \sum_{k=-\infty}^{+\infty} \left[J_k(A_1) e^{j\theta_1} + J_k(A_2) e^{-j\theta_2)} \right] e^{jk\omega_1 t} \\ &= \frac{1}{2} E_{in} \sum_{k=-\infty}^{+\infty} D_k e^{jk\omega_1 t} \end{aligned} \quad (6)$$

For a push-pull MZM excited by a sine-wave of which the expression is $S_3(t) = A_3 sin(\omega_2 t)$:

$$E_{out} = \frac{E_{in}}{2} \sum_{k=-\infty}^{+\infty} [J_k(A_3) + e^{-j\theta_3} J_k(-A_3)] e^{-jk\omega_2 t} \quad (7)$$

For odd values of *k*, $J_k(A_3) = -J_k(-A_3)$, for even values of *k*, $J_k(A_3) = J_k(-A_3)$. In the case were $\theta_3 = 0$, the expression of E_{out} becomes:

$$E_{out} = E_{in} \sum_{k=-\infty}^{+\infty} J_{2k}(A_3) e^{-jk\omega_2 t} \quad (8)$$

In the case where $\theta_3 \neq 0$, the expression of E_{out} becomes:

$$E_{out} = \frac{E_{in}}{2} \sum_{k=-\infty}^{+\infty} J_k(A_3)[1 + e^{-j\theta_3} \times (-1^k)] e^{-jk\omega_2 t} \quad (9)$$

knowing that $-1 = e^{j\pi}$, the expression is:

$$\begin{aligned} E_{out} &= \frac{E_{in}}{2} \sum_{k=-\infty}^{+\infty} J_k(A_3)[1 + e^{j(k\pi - \theta_3)}] e^{-jk\omega_2 t} \\ &= \frac{E_{in}}{2} \sum_{k=-\infty}^{+\infty} S_k e^{-jk\omega_2 t} \end{aligned} \quad (10)$$

The output spectrum of a dual arm MZM is symmetrical. Therefore, inverting the sign of *k* would lead to the same result.

$$E_{out} = \frac{E_{in}}{2} \sum_{k=-\infty}^{\infty} D_k e^{-jk\omega_1 t} \quad (11)$$

In the case of cascading MZMs, and due to their linearity wavelength-wise, each spectral ray generated by the first MZM is modulated by the second MZM to produce a copy of its response shifted by the spectral ray index. This operation is equivalent to a convolution. If we consider that $\omega_1 = \omega_2 = \omega$, the final output can be expressed as follows:

$$E_{out} = \frac{E_{in}}{2} \sum_{k=-\infty}^{+\infty} \underline{\mathrm{E}}_{out}[n] e^{-} jn\omega t \quad (12)$$

where $\underline{\mathrm{E}}_{out}[n]$ is the constant complex envelope of the n^{th} order harmonic considering the CW source's phase to be null:

$$\begin{aligned} \underline{E}_{out}[n] &= \frac{1}{2} |E_{in}| \sum_{k=-\infty}^{+\infty} D_k S_{n-k} \\ &= \frac{1}{2} |E_{in}| \sum_{k=-\infty}^{+\infty} \left[J_k(A_1) e^{j\theta_1} + J_k(A_2) e^{-j\theta_2} \right] \\ &\times J_{n-k}(A_3) \left[1 + e^{j((n-k)\pi - \theta_3)} \right] \end{aligned} \quad (13)$$

$$\begin{aligned} \underline{\mathrm{E}}_{out}[n] &= \frac{1}{2} |E_{in}| \sum_{k=-\infty}^{+\infty} J_k(A_1) J_{n-k}(A_3) \\ &\left[e^{j\theta_1} + e^{j((n-k)\pi - (\theta_3 - \theta_1))} \right] + J_k(A_2) J_{n-k}(A_3) \\ &\times \left[e^{-j\theta_2} + e^{j((n-k)\pi - (\theta_3 + \theta_2))} \right] \end{aligned} \quad (14)$$

C. Optimization Algorithm

Owing to the non-closed form of equation (5), we relied on a global optimization method, to obtain a comb source satisfying the following constraints:

- maximizing the number of leveled harmonics for a given ripple value;
- respecting the nominal operational range of the driving signals;
- having an acceptable flatness coefficient.

In the frequency domain, E_{out} is expressed as follows:

$$F(E_{out}) = \sum_{-\infty}^{+\infty} C_k \delta(k\omega_0) \quad (15)$$

This article has been accepted for publication in a future issue of this journal, but has not been fully edited. Content may change prior to final publication. Citation information: DOI 10.1109/JLT.2016.2636442, Journal of Lightwave Technology

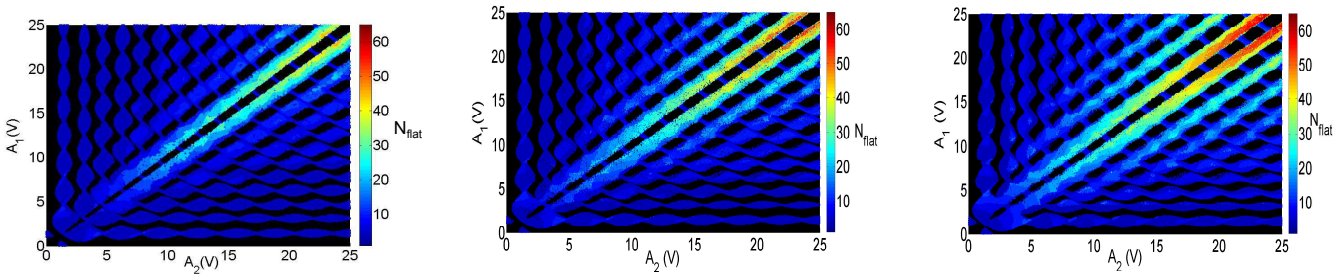

Fig. 3. The impact of RF generated phase-shift amplitudes A_1 and A_2 on the number of optical frequency harmonics in the flat optical comb N_{flat} for (a) $\Delta P = 1dB$, (b) $\Delta P = 2dB$ and (c) $\Delta P = 3dB$.

with C_k being the magnitudes of the harmonics observed at the output with the excitation signals $S_1(t)$ and $S_2(t)$, as depicted in Fig.1:

$$C_k = \frac{1}{2} E_{in} \left[J_k(A_1) e^{j\Delta\theta} + J_k(A_2) e^{-j\Delta\theta} \right] \tag{16}$$

In order to have N harmonics of equal power in the frequency comb for a given mean output optical power level $\bar{P}$ (mean output optical power level of the flat region), the following conditions must be respected:

$$\begin{cases} \left| \|C_k\|^2 - \bar{P} \right| \leq \Delta P & \forall \ \text{k} \quad \in]\frac{-N}{2}, \frac{N}{2}] \\ \left| \|C_k\|^2 - \bar{P} \right| \geq \Delta P & otherwise \end{cases} \tag{17}$$

where ΔP is the maximum permitted ripple. For multiple flat regions, the condition is generalized as follows:

$$\begin{cases} \arg\ max_j \left| \|C_{j,k}\|^2 - \overline{P}_j \right| \leq \Delta P & \forall \ \text{k} \in [-\frac{N}{2}, \frac{N}{2}] \\ \arg\ min_j \left| \|C_{j,k}\|^2 - \overline{P}_j \right| > \Delta P & \text{otherwise} \end{cases} \tag{18}$$

where *j* denotes the region of the output spectrum where the spectrum is flat within ΔP ripple. These regions must not overlap, and their flatness need not be global, i.e their mean power $\bar{P}_j$ is local to the region they belong to. The different regions are determined using a linear search on the vector $C = [\ldots, C_k, C_{k+1}, \ldots]$.

Due to the large search space, we applied an optimization algorithm. Simulated Annealing (SA) [22] was selected due to its faster convergence speed compared to a genetic algorithm-based approaches, which we did consider first. Simulated annealing is a local search algorithm which was inspired from the annealing in metalwork, like in heating and cooling a material to alter its internal structure for the purpose of enhancing its mechanical and tensile properties.

As in our case the problem involves two inequalities, with the second one (exclusivity condition) being the less important. We have chosen a weighted objective function:

$$\arg\ max_j F_j(\hat{k}_j, \Delta P) = \alpha \hat{k}_j^2 + (1-\alpha)\Delta P \tag{19}$$

where $\alpha \in [0, 1]$ is a tuning parameter, $\hat{k}_j$ is the harmonic number that falls within the range *P* for the region indexed *j*. The tuning parameter α defines the affinity of the algorithm either for minimizing ΔP or getting larger flat regions that fall within ΔP ripple.

D. Numerical results

Using the technique proposed by Sakamoto *et al.*, an 11 subcarriers frequency comb source was generated with a 1.1dB spectral ripple. The amplitude of the sine-waves A_1 and A_2 are equal to $25\pi/4$ and $23\pi/4$ based on a mono-tone excitation technique, as illustrated in Fig.2. In order to obtain a super-flat optical flat comb source, the proposed technique was optimized and simulated for the spectral flatness condition $\Delta P = 1$dB, $\Delta P = 2$dB and $\Delta P = 3$dB.

Fig.3 presents the mapping between A_1 and A_2 and the number of the flat harmonic N_{flat} for a spectral ripple equal to 1dB, 2dB and 3dB. The obtained results lead to conclude that the distribution of the spectral width is symmetrical in regard to A_1 and A_2, and the regions with the highest spectral width are located around the symmetry axis. Higher values of A_1 and A_2 are correlated with the number of flat harmonics. The radio frequency induced phase-shift $\phi_1(t)$ and $\phi_2(t)$ are relatively close for high harmonics number with a spectral flatness equal to 1dB. By increasing the tolerated spectral ripple ΔP to 3dB, the number of spectral lines increases.

Based on the optimized results, we propose a new flatness condition which replaces the condition presented in [21] (Eq. (5)), described as follows:

$$|\Delta A| \pm \Delta\theta = \pm k \frac{\pi}{4} \tag{20}$$

In [21] Sakamoto *et al.* have generated 11 spectral lines using large amplitude sine-waves ($A_1 = 23\pi/4$ and $A_2 = 25\pi/4$) with 1.1dB spectral ripple. Using a global optimization method, we generated 11 spectral lines with an optimal operational input range A_1 and A_2 equal to $10.2\pi/4$ and $11.7\pi/4$, respectively, and a spectral flatness condition $\Delta P = 1$dB.

We point out that we can generate 4, 8, 16 and 32 spectral lines. The optimized driving condition with $\Delta P = 1dB$ for different flat harmonic values are summarized in Table I.

TABLE I
THE OPTIMAL DRIVEN CONDITION WITH $\Delta P = 1dB$ FOR 4, 8, 16 AND 32 VALUES USING DUAL ARM MZM

N_{flat}	4	8	16	32
A_1	$8.1\pi/4$	$9.6\pi/4$	$14.6\pi/4$	$39.4\pi/4$
A_2	$12.5\pi/4$	$11.1\pi/4$	$16.2\pi/4$	$38.1\pi/4$
$\Delta\theta$	$5.3\pi/4$	$5.5\pi/4$	$10.2\pi/4$	$13.3\pi/4$
$\Delta P(dB)$	0.3	0.5	0.65	0.9

This article has been accepted for publication in a future issue of this journal, but has not been fully edited. Content may change prior to final publication. Citation information: DOI 10.1109/JLT.2016.2636442, Journal of Lightwave Technology

For a $\Delta P = 1$dB, we were able to obtain 4, 8, 16 and 32 new spectral lines in addition to the center wavelength (1552.52nm), as presented in Fig.4. The modulation frequency is 12.5 GHz. The amplitude of the RF signal S_1 and S_2 are obtained using the values given in Table I, replacing π by V_π with $V_\pi = 4V$ in our simulation.

The excitation frequency of the MZM is 12.5GHz with $V_\pi = 4V$. The nominal operational range A_1 and range A_2 of the driving signals are tuned from 0V to 25V (peak-to-peak amplitudes). In order to increase the number of spectral lines, a cascade of dual arm and push-pull Mach-Zehnder modulators are used.

In case of two-stage of MZM, we obtain 7, 12, 20 and 41 spectral lines with 1dB as spectral ripple using the optimized algorithm, as depicted in Fig.5. The optimized driving condition with $\Delta P = 1$dB for different harmonic values generated at the output of the two-stage of MZM is given in Table II.

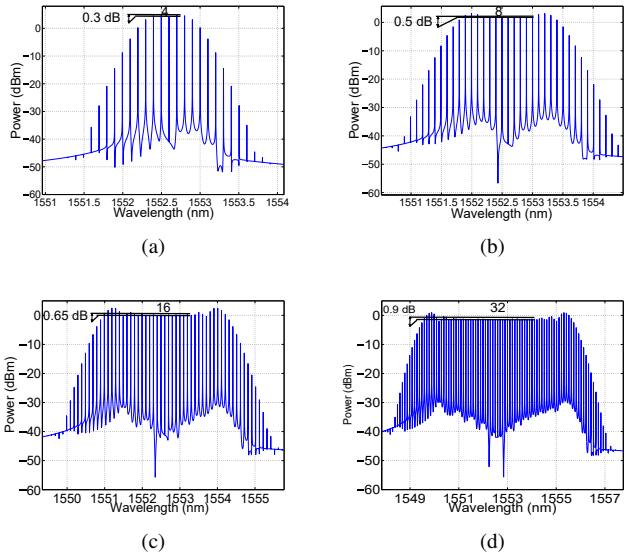

Fig. 4. Simulated output spectrum using a dual drive MZM with different driving conditions for (a) $N_{flat} = 4$ ($A_1 = 8.1\pi/4$, $A_2 = 12.5\pi/4$), (b) $N_{flat} = 8$ ($A_1 = 9.6\pi/4$, $A_2 = 11.1\pi/4$), (c) $N_{flat} = 16$ ($A_1 = 14.6\pi/4$, $A_2 = 16.2\pi/4$) and (d) $N_{flat} = 32$ ($A_1 = 39.4\pi/4$, $A_2 = 38.1\pi/4$), with spectral ripple less than 1dB, optimized by applying the optimization algorithm

TABLE II
THE OPTIMAL DRIVEN CONDITION WITH $\Delta P = 1dB$ FOR 7, 12, 20 AND 41 VALUES USING TWO-STAGE OF MZM

N_{flat}	7	12	20	41
A_1	$9.1\pi/4$	$10.2\pi/4$	$15\pi/4$	$39.7\pi/4$
A_2	$10.3\pi/4$	$8\pi/4$	$16.6\pi/4$	$38.6\pi/4$
A_3	$2.2\pi/4$	$6\pi/4$	$11.5\pi/4$	$26.2\pi/4$
$\Delta\theta_1$	$6.6\pi/4$	$7\pi/4$	$13.2\pi/4$	$18.5\pi/4$
θ_3	$4\pi/4$	$6\pi/4$	$\pi/4$	$10\pi/4$
$\Delta P(dB)$	0.58	0.8	0.9	1

III. EXPERIMENTAL SETUP FOR OPTICAL FLAT COMB SOURCE GENERATION

Fig. 6 shows the experimental design of an OFCS based on dual arm Mach-Zehnder modulator (stage 1). The narrow

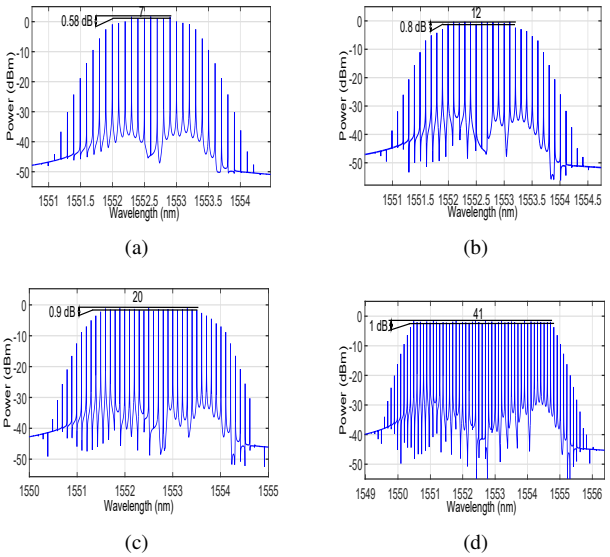

Fig. 5. Simulated output spectrum using two stage MZM with different driving conditions for (a) $N_{flat} = 7$ ($A_1 = 9.1\pi/4$, $A_2 = 10.3\pi/4$, $A_3 = 2.2\pi/4$), (b) $N_{flat} = 12$ ($A_1 = 10.2\pi/4$, $A_2 = 8\pi/4$, $A_3 = 6\pi/4$), (c) $N_{flat} = 20$ ($A_1 = 15\pi/4$, $A_2 = 16.6\pi/4$, $A_3 = 11.5\pi/4$) and (d) $N_{flat} = 41$ ($A_1 = 39.7\pi/4$, $A_2 = 38.6\pi/4$, $A_3 = 26.2\pi/4$), with spectral ripple less than $1dB$, optimized by applying the optimization algorithm

linewidth 1552.5 nm continuous wave (CW) optical carrier is generated by an external cavity laser (ECL) and is modulated by the DA-MZM. The DA-MZM ($AT\&Tm2122CA$ with a single drive $V_\pi = 4V$) is driven by a sinusoidal RF signal at a frequency f_1 equal to 6.25GHz. The driving signals A_1 and A_2 are generated by two Photline drivers $DR - AN - 20 - MO$. The obtained results are visualized on a high resolution $APEXAP2050A$ optical spectrum analyzer (OSA).

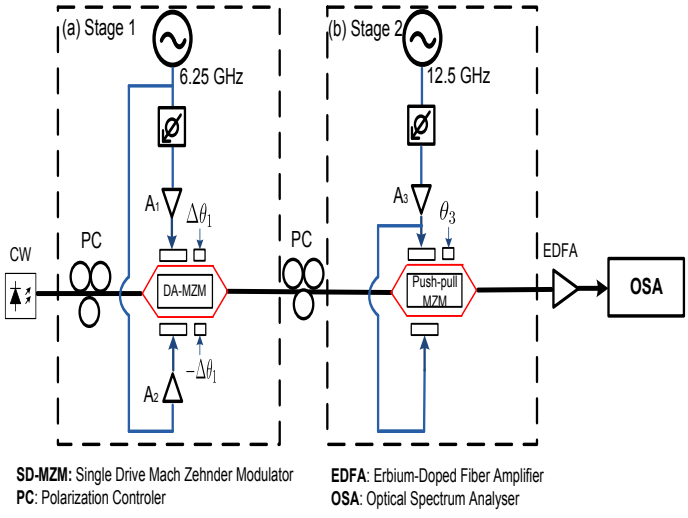

Fig. 6. Experimental set-up for generating an Optical Flat Comb Source.

Due to the limited output power of the available amplifiers, we experimentally generated 7 spectral lines with a spectral ripple equal to 0.86dB, as illustrated in Fig.7. In order to increase the number of spectral lines, we used a second stage composed by a push-pull MZM (Photline $MX - LN - 10$)

This article has been accepted for publication in a future issue of this journal, but has not been fully edited. Content may change prior to final publication. Citation information: DOI 10.1109/JLT.2016.2636442, Journal of Lightwave Technology

with a single drive $V_\pi = 4V$) driven by a sinusoidal RF signal at a frequency f_2 equal to 12.5GHz. The push-pull MZM is used to increase the number of subcarrier. In the output of the second stage, we generated 11 spectral lines with a spectral ripple equal to 1dB, as depicted in Fig.8.

The optimal experimental driven condition for different flat harmonic values (7, 9 and 11) are presented in Table III.

It is important to mention that The value of the amplitude of RF signals (A_1, A_2 and A_3) which are presented in table II are higher than the values indicated in table III. Using the optimization algorithm, we obtain a range of values. Due to the limited output power of the available amplifier, we used the lower amplitude of the RF signal S_1 and S_2 which are non-mentioned in table II.

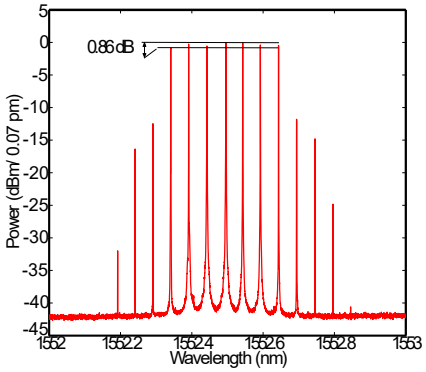

Fig. 7. Experimental output spectrum with different driving conditions for $N_{flat} = 7$ with spectral ripple less than 1dB at the output of the 1^{st} stage.

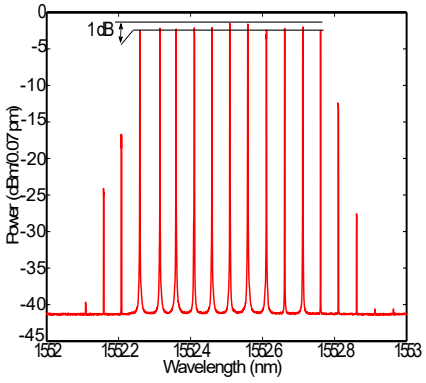

Fig. 8. Experimental output spectrum with different driving conditions for $N_{flat} = 11$ with spectral ripple equal to 1dB at the output of the 2^{nd} stage.

TABLE III
THE OPTIMAL EXPERIMENTAL DRIVEN CONDITION WITH $\Delta P = 1dB$ FOR 7, 9 AND 11 SUBCARRIERS

N_{flat}	A_1	A_2	A_3	$\Delta\theta$	θ_3	ΔP
7	$0.7\pi/4$	$3.5\pi/4$	$\pi/4$	$8\pi/4$	$4\pi/4$	0.75
9	$0.9\pi/4$	$4.3\pi/4$	$2.3\pi/4$	$4\pi/4$	$5.2\pi/4$	0.85
11	$1.5\pi/4$	$5\pi/4$	$3.7\pi/4$	$2.7\pi/4$	$6\pi/4$	1

IV. 16QAM-OFDM UDWDM PON USING A TUNABLE OPTICAL FLAT COMB SOURCE

In order to demonstrate the flexibility and the feasibility of the OFCS, which is based on a cascade of two MZMs, we used the OFCS for 16QAM-OFDM transmission ($11 \times 12.5Gbps$)with direct detection over 25km and 100km SSMF fiber, as illustrated in Fig. 9.

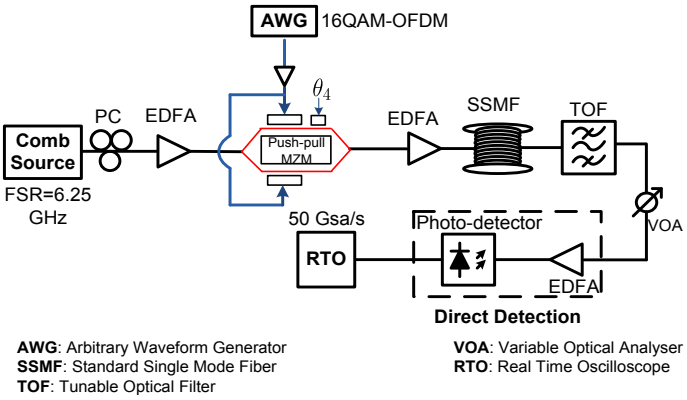

Fig. 9. Experimental setup of 16QAM-OFDM UDWDM PON signal generation based on optical flat comb source using direct detection.

The numerical OFDM modulating signal is generated with Matlab. It consists of 300 OFDM symbols, each one of them is generated as follows: 256 at the input of the IFFT arranged to have Hermitian symmetry in order to get a real-valued base band OFDM signal. Analog OFDM signal is generated with an arbitrary waveform generator (AWG) at 12 GSymbols/s. The signal is injected to the push pull-MZM. The real-valued baseband OFDM signal is composed of 64 subcarriers occupying a total 3GHz bandwidth. Each OFDM subcarrier is modulated by a 16QAM constellation and 8 samples per symbol are used as a cyclic prefix (CP). The optical signal for each optical subcarrier is a double-side band thus occupying a 6GHz band each.

The OFDM signal is amplified by a RF Photline amplifier $DR-GA-10$. The optical signal is transmitted over a short link in back-to-back and over 25km and 100km of SSMF fiber.The launch power into the transmission fiber is equal to 0 dBm (1mW). At the receiver, the signal is pre-amplified and filtered in order to reduce the amplified spontaneous emission (ASE) using a high order Gaussian optical band-pass filter (OBPF). The tunable filter ($YenistaXTA-50Ultrafine$) is characterized by Wavelength tuning range over 1480 to 1620nm and an edge roll-off of 800 dB/nm. In addition, the bandwidth setting range of the optical filter is over 32 to 650 pm. The actual filter bandwidth used in the experiments is equal to 6.25 GHz (50pm). We notes that, the use of this filter allows us to experimentally set up and evaluate the proof of concept of the proposed UDWDM-PON architecture. A real system would use WDM demultiplexer such as an arrayed waveguide grating (AWG) [23], [24] or a bulk demultiplexer such as Kylia's athermal DEMUX tunable [25] instead for filtering and addressing the wavelength channels.

The optical signal is converted to an electrical signal using 10GHz (PIN) photo-detector (PD). The analog conversion is done by means of a real time oscilloscope (RTO) Tektronik $DPO72004B$The OFDM signals are processed offline using Matlab.

It is important to mention that at this stage we have just

This article has been accepted for publication in a future issue of this journal, but has not been fully edited. Content may change prior to final publication. Citation information: DOI 10.1109/JLT.2016.2636442, Journal of Lightwave Technology

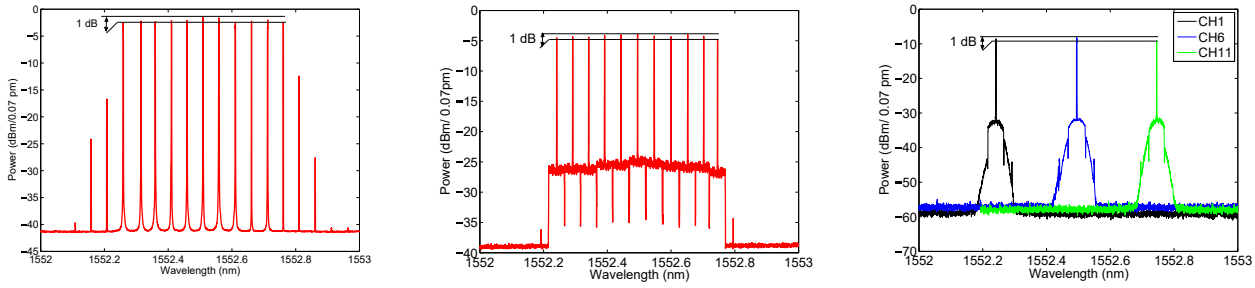

(a) (b) (c)

Fig. 10. (a) Experimental output spectrum of 11 subcarriers with a spectral ripple $\Delta P = 1dB$ equal to 1dB, (b) the optical spectrum of the modulated carriers and (c) the optical spectrum of the 3 filtered channels (CH1, CH6 and CH11).

worked on the transmitter architecture and the optical budget could be enhanced by increasing the power of the optical signal. The optical budget is the difference between the power boosted in the fiber and the lowest power received by the preamplifier.

The spectrum of the 11 generated carriers in the output of the OFCS which based on a cascade of two MZMs is illustrated in Fig. 10(a). The optical spectrum of the 11 modulated carriers is shown in Fig. 10(b). In this work, we demonstrate the performance of 3 channels (channel 1(CH1), channel 6(CH6) and channel 11(CH11)). We evaluate the performance of the three channels by carrying out EVM measurements in a back-to-back scenario and over uncompensated transmission links composed of 25km and 100km SSMF.

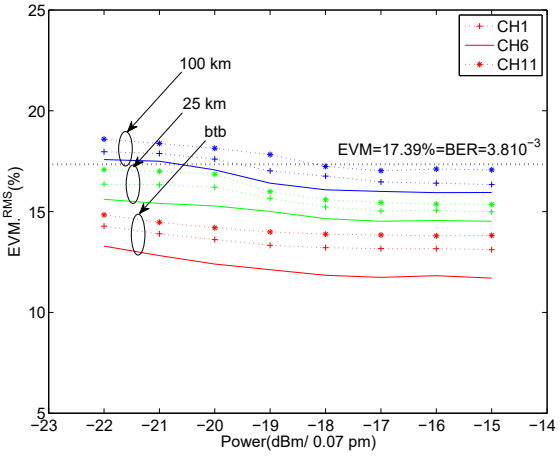

Fig. 11. Performance evaluation of the filtered channels (CH1, CH6 and CH11) in term of EVM in Back-to-Back scenario and over 25km and 100km SSMF link.

The three filtered channels (CH1, CH6 and CH11) demonstrate different performances in terms of receiver sensitivity. The channel 6 (CH6) has the best performance compared to CH1 and CH11. The penalty can mainly be due to the spectral ripple which is equal to 1dB. After a transmission distance equal to 100km of SSMF, CH1, CH6 and CH11 are below the bit error rates (BER) threshold for a received power equal to -21dBm, -20dBm and -18dBm, respectively. In Fig.11, the black dashed lines present the EVM corresponding to the BER threshold. For channel 6(CH6), which presents the best performance, we study the response channel and the EVM per subcarrier, as described in Fig.12. We find that the channel is constant and does not suffer from any fading effect.

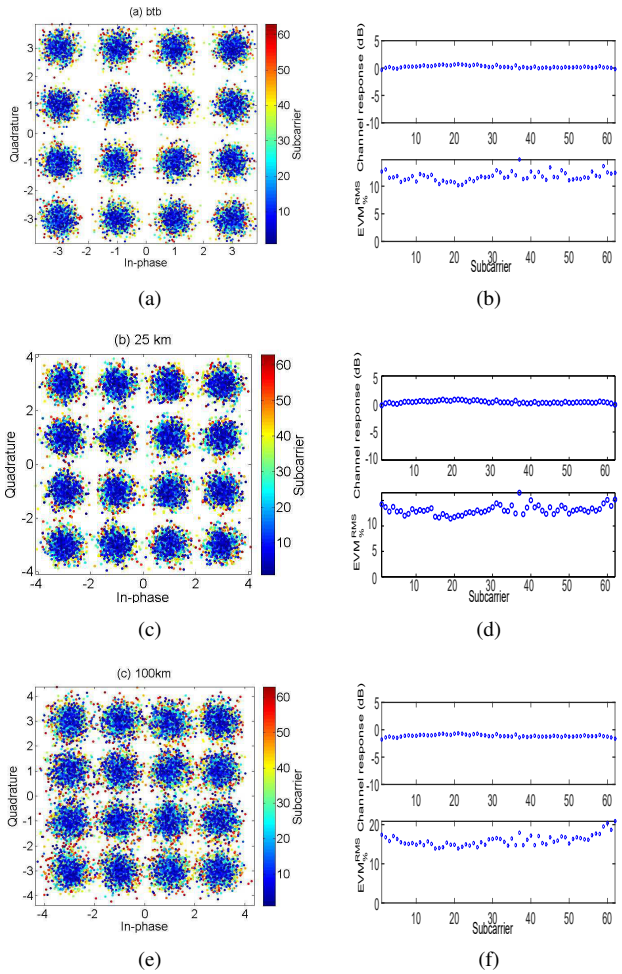

(a) (b) (c) (d) (e) (f)

Fig. 12. EVM per OFDM subcarrier and channel response for the filtred channel 6 (CH6) over uncompensated transmission link (0km, 25km and 100km) SSMF ($receivedpower = -18dBm$).

The absence of the fading in the channel 6 is mainly due to the perfect double side band generated signal which has good effects on the transmission performances. In addition, The frequency response of the channel 6 is constant which

highlight the absence of the chromatic dispersion effect. This is consistent with the small value of the bandwidth (equal to $\pm 3GHz$ on both side of each carrier) of the non-chirped OFDM-modulation obtained with a push-pull MZM and the length of the fiber. Single side-band modulation is not required here even for 100km length (even though using SSB could double the effective transmission rate) [26]. The EVM per OFDM subcarrier and channel response for the filtered CH6 is demonstrated for a received power equal to -18dBm. The total bit rate of the multiplex is $11 \times 12,5 = 137,5 Gbit/s$.

V. Conclusion

In this paper, we have demonstrated the efficiency of an OFCS in the generation of 16QAM-OFDM-UDWDM PON system. We have proven that a dual-arm MZM driven by a sinusoidal signal can generate 32 spectral lines with a spectral ripple equal to 1dB. Additionally, we have verified that the use of a cascade of two Mach-Zehnder modulators increase the number of the carriers to acheive 41 spactral lines. In our case, we have experimentally generated 11 subcarriers with a spectral ripple equal to 1dB due to the limited output power of the avaible amplifiers. Experiments have illustrated the transmission of 137,5Gbps ($11 \times 12.5 Gbps$) 16QAM-OFDM-UDWDM transmission over uncompensated transmission link of 25km and 100km using a direct detection. The incentive of the present work was to assess the validity of the transmitter architecture and to show how the optical budget could be enhanced by increasing the power of the optical signal. In order to evaluate the performance of the filtered channels in terms of error vector magnitude, a sharp tunable filter is used in our experiment. In the future, an AWG DEMUX with 6.25 GHz spacing will be more suitable for designing a low cost PON access system. In addition, providing a decorrelation stage after the modulation can enhance the performance of the UDWDM PON system.

References

[1] J. K. Fischer, M. Nölle, L. Molle, C. Schmidtlanghorst, J. Hilt, R. Ludwig, and C. Schubert, "Beyond 100g-high-capacity transport technologies for next generation optical core networks," in *Future Network & Mobile Summit (FutureNetw), 2012*. IEEE, 2012, pp. 1–9.

[2] D. Nesset, "Ng-pon2 technology and standards," *Journal of Lightwave Technology*, vol. 33, no. 5, pp. 1136–1143, 2015.

[3] S. Smolorz, H. Rohde, E. Gottwald, D. W. Smith, and A. Poustie, "Demonstration of a coherent udwdm-pon with real-time processing," in *National Fiber Optic Engineers Conference*. Optical Society of America, 2011, p. PDPD4.

[4] R. Ferreira, J. D. Reis, S. M. Rossi, S. B. Amado, A. Shahpari, N. G. Gonzalez, J. R. Oliveira, A. N. Pinto, and A. L. Teixeira, "Demonstration of nyquist udwdm-pon with digital signal processing in real-time," in *Optical Fiber Communication Conference*. Optical Society of America, 2015, pp. Th3I–4.

[5] A. Shahpari, R. Ferreira, V. Ribeiro, A. Sousa, S. Ziaie, A. Tavares, Z. Vujicic, F. P. Guiomar, J. D. Reis, A. N. Pinto *et al.*, "Coherent ultra dense wavelength division multiplexing passive optical networks," *Optical Fiber Technology*, vol. 26, pp. 100–107, 2015.

[6] P. M. Anandarajah, R. Zhou, V. Vujicic, D. Gutierrez Pascual, E. Martin, and L. P. Barry, "Long reach udwdm pon with scm-qpsk modulation and direct detection," in *Optical Fiber Communication Conference*. Optical Society of America, 2014, pp. W2A–42.

[7] P. M. Anandarajah, T. N. Huynh, V. Vujicic, R. Zhou, and L. P. Barry, "Udwdm pon with 6 x 2.5 gbaud 16-qam multicarrier transmitter and phase noise tolerant direct detection," in *Optical Fiber Communication Conference*. Optical Society of America, 2015, pp. Th2A–58.

[8] P. M. Anandarajah, T. Shao, R. Zhou, D. Gutierrez Pascual, and L. P Barry, "100gb/s wdm-ssb-dd-ofdm using a gain switched monolithically integrated passive feedback comb source," in *CLEO: Science and Innovations*. Optical Society of America, 2015, pp. SF2K–1.

[9] V. Sales, J. Segarra, V. Polo, J. C. Velásquez, and J. Prat, "Udwdm-pon using low-cost coherent transceivers with limited tunability and heuristic dwa," *Journal of Optical Communications and Networking*, vol. 8, no. 8, pp. 582–599, 2016.

[10] V. Ataie, E. Temprana, L. Liu, E. Myslivets, B. P.-P. Kuo, N. Alic, and S. Radic, "Ultrahigh count coherent wdm channels transmission using optical parametric comb-based frequency synthesizer," *Journal of Lightwave Technology*, vol. 33, no. 3, pp. 694–699, 2015.

[11] Z. Dong, H.-C. Chien, J. Yu, J. Zhang, L. Cheng, and G.-k. Chang, "Very-high-throughput coherent ultradense wdm-pon based on nyquist-isb modulation," *Photonics Technology Letters, IEEE*, vol. 27, no. 7, pp. 763–766, 2015.

[12] H. Takara, T. Ohara, K. Mori, K. Sato, E. Yamada, Y. Inoue, T. Shibata, M. Abe, T. Morioka, and K. Sato, "More than 1000 channel optical frequency chain generation from single supercontinuum source with 12.5 ghz channel spacing," *Electronics Letters*, vol. 36, no. 25, p. 1, 2000.

[13] F.-L. Hong, K. Minoshima, A. Onae, H. Inaba, H. Takada, A. Hirai, H. Matsumoto, T. Sugiura, and M. Yoshida, "Broad-spectrum frequency comb generation and carrier-envelope offset frequency measurement by second-harmonic generation of a mode-locked fiber laser," *Optics letters*, vol. 28, no. 17, pp. 1516–1518, 2003.

[14] R. Wu, V. Supradeepa, C. M. Long, D. E. Leaird, and A. M. Weiner, "Generation of very flat optical frequency combs from continuous-wave lasers using cascaded intensity and phase modulators driven by tailored radio frequency waveforms," *Optics letters*, vol. 35, no. 19, pp. 3234–3236, 2010.

[15] I. L. Gheorma and G. K. Gopalakrishnan, "Method and system for generating flat or arbitrary shaped optical frequency combs," May 31 2011, uS Patent 7,953,303.

[16] Y. Ma, Q. Yang, Y. Tang, S. Chen, and W. Shieh, "1-tb/s single-channel coherent optical ofdm transmission with orthogonal-band multiplexing and subwavelength bandwidth access," *Lightwave Technology, Journal of*, vol. 28, no. 4, pp. 308–315, 2010.

[17] C. Weimann, P. Schindler, R. Palmer, S. Wolf, D. Bekele, D. Korn, J. Pfeifle, S. Koeber, R. Schmogrow, L. Alloatti *et al.*, "Silicon-organic hybrid (soh) frequency comb sources for terabit/s data transmission," *Optics express*, vol. 22, no. 3, pp. 3629–3637, 2014.

[18] X. Zhou, X. Zheng, H. Wen, H. Zhang, and B. Zhou, "Generation of broadband optical frequency comb with rectangular envelope using cascaded intensity and dual-parallel modulators," *Optics Communications*, vol. 313, pp. 356–359, 2014.

[19] J. Zhang, J. Yu, N. Chi, Z. Dong, X. Li, Y. Shao, J. Yu, and L. Tao, "Flattened comb generation using only phase modulators driven by fundamental frequency sinusoidal sources with small frequency offset," *Optics letters*, vol. 38, no. 4, pp. 552–554, 2013.

[20] C. Chen, C. He, D. Zhu, R. Guo, F. Zhang, and S. Pan, "Generation of a flat optical frequency comb based on a cascaded polarization modulator and phase modulator," *Optics letters*, vol. 38, no. 16, pp. 3137–3139, 2013.

[21] T. Sakamoto, T. Kawanishi, and M. Izutsu, "Widely wavelength-tunable ultra-flat frequency comb generation using conventional dual-drive mach-zehnder modulator," *Electronics Letters*, vol. 43, no. 19, pp. 1039–1040, 2007.

[22] P. J. Van Laarhoven and E. H. Aarts, *Simulated annealing: theory and applications*. Springer Science & Business Media, 1987, vol. 37.

[23] T. Ohara, H. Takara, T. Yamamoto, H. Masuda, T. Morioka, M. Abe, and H. Takahashi, "Over-1000-channel ultradense wdm transmission with supercontinuum multicarrier source," *Journal of lightwave technology*, vol. 24, no. 6, p. 2311, 2006.

[24] J. D. Reis, D. M. Neves, and A. L. Teixeira, "Physical impairments on high aggregate data rate passive coherent optical networks," in *Microwave & Optoelectronics Conference (IMOC), 2011 SBMO/IEEE MTT-S International*. IEEE, 2011, pp. 366–370.

[25] Kylia, "Dwdm mux/demux," *http://kylia.com/kylia/?portfoliomuxdemux-mics-tmics*.

[26] M. E. Chaibi, D. Erasme, T. Anfray, C. Aupetit-Berthelemot, and C. Kazmierski, "Generation of ssb optical signals with dual-eml modulated with wideband ofdm," in *CLEO: Science and Innovations*. Optical Society of America, 2014, pp. SW1J–6.